0013-7227/04/$15.00/0
Printed in U.S.A.

Endocrinology 145(7):3205–3214

doi: 10.1210/en.2003-1716

Saw Palmetto Extract Suppresses Insulin-Like Growth Factor-I Signaling and Induces Stress-Activated Protein Kinase/c-Jun N-Terminal Kinase Phosphorylation in Human Prostate Epithelial Cells

TERI L. WADSWORTH, JULIE M. CARROLL, REBECCA A. MALLINSON, CHARLES T. ROBERTS, JR., AND CHARLES E. ROSELLI

Departments of Physiology and Pharmacology (T.L.W., C.E.R.) and Pediatrics (J.M.C., C.T.R.), Oregon Health and Science University, Portland, Oregon 97239

A common alternative therapy for benign prostatic hyperplasia (BPH) is the extract from the fruit of saw palmetto (SPE). BPH is caused by nonmalignant growth of epithelial and stromal elements of the prostate. IGF action is important for prostate growth and development, and changes in the IGF system have been documented in BPH tissues. The main signaling pathways activated by the binding of IGF-I to the IGF-I receptor (IGF-IR) are the ERK arm of the MAPK cascade and the phosphoinositol-3-kinase (PI3K)/protein kinase B (PKB/Akt) cascade. We tested the hypothesis that SPE suppresses growth and induces apoptosis in the P69 prostate epithelial cell line by inhibiting IGF-I signaling. Treatment with 150 μg/ml SPE for 24 h decreased IGF-I-induced proliferation of P69 cells and induced cleavage of the enzyme poly(ADP-ribose)polymerase (PARP), an index of apoptosis. Treatment of serum-starved P69 cells with 150 μg/ml SPE for 6 h reduced IGF-I-induced phosphorylation of Akt (assessed by Western blot) and Akt activity (assessed by an Akt kinase assay). Western blot analysis showed that SPE reduced IGF-I-induced phosphorylation of the adapter protein insulin receptor substrate-1 and decreased downstream effects of Akt activation, including increased cyclin D1 levels and phosphorylation of glycogen synthase kinase-3 and $p70^{s6k}$. There was no effect on IGF-I-induced phosphorylation of MAPK, IGF-IR, or Shc. Treatment of starved cells with SPE alone induced phosphorylation the proapoptotic protein JNK. SPE treatment may relieve symptoms of BPH, in part, by inhibiting specific components of the IGF-I signaling pathway and inducing JNK activation, thus mediating antiproliferative and proapoptotic effects on prostate epithelia. (*Endocrinology* 145: 3205–3214, 2004)

BENIGN PROSTATIC HYPERPLASIA (BPH), a nonmalignant growth of the epithelial and stromal elements of the prostate gland, is an extremely common condition in elderly men. The progression of BPH is thought to be dependent on a combination of growth factors, adrenergic stimulation, inflammatory processes, and the 5α-reductase-mediated conversion of testosterone to dihydrotestosterone (DHT) (1, 2). IGF action has been shown to be particularly important for prostate growth and development, and changes in the IGF system have been previously documented in prostate stromal cell lines derived from BPH patients *vs.* controls (3–5).

The main signaling pathways activated by the binding of IGF-I to the IGF-I receptor (IGF-IR) in prostate and other cell types are the ERK arm of the MAPK cascade and the phosphoinositol-3-kinase (PI3K)/protein kinase B (PKB/Akt) cascade (6). The activated IGF-IR is coupled to the ERK pathway via adapter proteins of the insulin receptor substrate (IRS) and Shc families, which culminate in the activation of the extracellular signal-related kinases ERK1 and ERK2. Subsequent phosphorylation and activation of transcription factors trigger changes in gene expression patterns that result in mitogenic or differentiative cellular responses (7). IRS and, potentially, Shc proteins also couple the active receptor to the p85 regulatory subunit of PI3K. Subsequent generation of the second messenger phosphotidylinositol 3-phosphate on the inner plasma membrane by PI3K recruits Akt via interaction with its pleckstrin homology (PH) domain. Simultaneously, phosphoinositide-dependent kinase 1 (PDK1) phosphorylates Akt on Thr 308. Maximal activation of Akt requires additional phosphorylation at Ser 473 by an as-yet poorly characterized kinase termed PDK2 (6, 8). Downstream effects of PI3K/Akt activation include protection from apoptosis and increased cellular proliferation due, in part, to phosphorylation and inhibition of proteins such as glycogen synthase kinase-3β (GSK-3β) and phosphorylation and activation of proteins such as p70S6 kinase ($p70^{S6K}$) (8, 9). Phosphorylation of cyclin D1 by GSK-3β triggers the redistribution of cyclin D1 from the nucleus to the cytoplasm, where it is targeted for ubiquitin-dependent proteolysis. Phosphorylation/inactivation of GSK3β by Akt, therefore, results in elevated levels of cyclin D1, thus allowing progression through the G1 phase of the cell cycle. Akt also

Abbreviations: AR, Androgen receptor; BAD, Bcl-2 agonist of cell death; BPH, benign prostatic hyperplasia; CaP, prostate cancer; DHT, dihydrotestosterone; FKHR, forkhead transcription factor; GSK-3β, synthase kinase-3β; IGF-IR, IGF-I receptor; IRS, insulin receptor substrate; JNK, c-Jun N-terminal kinase; MTS, carboxymethyphenyl-2-(4-sulphophenyl)-2H-tetrazolium, inner salt; PARP, poly(ADP-ribose)polymerse; PDK, phosphoinositide-dependent kinase; PI3K, phosphoinositol-3-kinase; PKB/Akt, protein kinase A; SAPK, stress-activated protein kinase; SDS, sodium dodecyl sulfate; SPE, fruit of saw palmetto.

***Endocrinology* is published monthly by The Endocrine Society (http://www.endo-society.org), the foremost professional society serving the endocrine community.**

increases cyclin D1 levels by stimulating mRNA translation (10–12). In response to IGF-I stimulation, $p70^{S6K}$ can be directly phosphorylated by PDK1 or indirectly phosphorylated by downstream Akt signaling. $p70^{S6K}$ is thought to regulate cell growth by participating in the translation of mRNAs containing a 5′-oligopyrimidine tract, and it has also been shown to phosphorylate and inactivate the proapoptotic protein Bcl-2 agonist of cell death (BAD) (13, 14).

Although apoptosis may be activated by inhibiting the effects of growth factors, it can also be triggered by proapoptotic stimuli such as proinflammatory cytokines and ceramides that phosphorylate and activate the stress-activated protein kinase (SAPK)/c-Jun N-terminal kinase (JNK) (15, 16). SAPK/JNK exhibits inhibitory effects on insulin signaling in 32D cells and IGF-I signaling in breast cancer cells. By phosphorylating Ser 312 of human IRS-1 (which lies adjacent to its protein tyrosine binding domain), SAPK/JNK is thought to inhibit IGF-I and insulin signaling pathways by preventing binding of IRS to the IGF-IR and insulin receptors (17–19). In addition to activating transcription factors such as c-Jun, activated SAPK/JNK can also inactivate the antiapoptotic protein Bcl-2 (20).

Over the past 10 yr, dissatisfaction with side effects from conventional treatments such as the 5α-reductase inhibitor finasteride and α-adrenergic blockers, the need for personal control, and a philosophical congruence between alternative therapies and patient values has led to an increased popularity of self-medication with herbal medicines to treat the symptoms of BPH (21–23). Extract from the fruit of saw palmetto (*Serenoa repens*, a shrubby palm native to North America) is prescribed routinely in Europe to relieve the symptoms of BPH. In the United States, where herbal medicines are available as nonprescription dietary supplements, saw palmetto extract (SPE) is the most common herb used to promote prostate health. Randomized studies have provided evidence for the tolerability and efficacy of SPE in treating BPH symptoms (24). SPE is a complex mixture composed of saturated and unsaturated fatty acids, sterols, flavonoids, and alcohols. Multiple mechanisms of action have been proposed for SPE, including inhibition of 5α-reductase, inhibition of DHT binding to the androgen receptor (AR), antiinflammatory effects mediated by the inhibition of cyclooxygenase and lipoxygenase, and inhibition of fibroblast and epidermal growth factor-induced prostate cell proliferation (23, 25, 26). SPE has been shown to induce mixed cell death due to apoptosis and necrosis in the LNCaP prostate cancer cell line, to inhibit proliferation and induce apoptosis in human BPH tissues, and to decrease basal expression of Bcl-2 in Jurkat cells (26–28).

In this study, we tested the hypothesis that SPE suppresses prostate epithelial cell growth and induces apoptosis by inhibiting IGF-I signaling. We also investigated the effects of SPE on SAPK/JNK activity. Our *in vitro* model for BPH was the poorly tumorigenic, nonmetastatic, simian virus 40 T antigen-immortalized P69 prostate epithelial cell line (29). Because P69 cells do not express the AR (30), effects of SPE on this cell line are independent of its potential effects on 5α-reductase or binding of DHT to the AR.

Materials and Methods

Materials

Bright-Line hemocytometer was from American Optical (Buffalo, NY). Bio-Rad DC Protein Assay and Molecular Analyst software were from Bio-Rad Laboratories (Hercules, CA). Rabbit antisera specific for phospho-IGF-IR was from Biosource (Camarillo, CA). Rabbit antisera specific for phospho-Akt (Ser 473 and Thr 308), Akt, phospho-GSK-3β (Ser 9), phospho-forkhead transcription factor (FKHR) (Ser 256), phospho-BAD (Ser 136), phospho-IRS-1 (Ser 307), IRS-1, phospho-p44/42 ERK, phospho-Shc, and p42 ERK, and the Nonradioactive Akt Kinase Assay Kit were from Cell Signaling Technologies (Beverly, MA). Receptor-grade IGF-I was from GroPep, Ltd. (North Adelaide, Australia). SPE (*Serenoa repens* purified extract, Sabalselect) was from Indena s.a. (Tours, France). Gentamicin, insulin-transferrin-selenium, serum-free RPMI, Dulbecco's PBS, fungizone, and recombinant human epidermal growth factor were from Invitrogen Life Technologies (Carlsbad, CA). Propidium iodide was from Molecular Probes (Eugene, OR). Supersignal7 Ultra chemiluminescent substrate was from Pierce Biotechnology (Rockford, IL). CellTiter 96 Aq_{ueous} Nonradioactive Cell Proliferation kit was from Promega Corp. (Madison WI). Rabbit antisera specific phospho-JNK (G7), JNK1 (FL), IGF-IRβ (C-20), Bcl-2, IGF-IR, and poly(ADP-ribose)polymerase (PARP) (H-250), and mouse antisera specific for cyclin D1 and phosphotyrosine 20 were from Santa Cruz Biotechnology (Santa Cruz, CA). Rabbit antisera specific for IRS-1 were from Upstate (Charlottesville, VA). Nitrocellulose membranes were from Schleicher & Schuell (Keene, NH). Dexamethasone, Triton X-100, ribonuclease A, and monoclonal mouse anti-α-tubulin were from Sigma-Aldrich (St. Louis, MO). Rabbit antisera specific for Shc were from Transduction Laboratories (Lexington, KY). The UVP Bioimaging System and LabWorks 4.0 Image Acquisition Software were from UVP, Inc. (Upland, CA).

Cell culture

P69 cells were cultured in a defined medium composed of phenol red-free RPMI supplemented with 10 ng/ml epidermal growth factor, 10 μg/ml gentamycin, 0.2 μM dexamethasone, 10 μg/ml insulin, 5.5 μg/ml transferrin, 6.7 ng/ml sodium selenite, and 2.5 μg/ml fungizone. Starvation media consisted of phenol red-free RPMI. Cells were maintained in a tissue culture incubator at 37 C in humidified air containing 5% CO_2.

Treatments

SPE was dissolved in ethanol to give a concentrated stock solution and centrifuged at 12,000 × *g* for 5 min to remove insoluble debris. Aliquots of stock solution and/or ethanol were added to starvation media at 37 C to give the final desired concentrations of SPE and a final ethanol concentration of 0.5%. The solutions were vigorously vortexed for 3 min, rewarmed to 37 C, and added to the cells. IGF-I (50 nM) was added for 10 min.

Western blots

Cells were plated into six-well flasks at a density of 4×10^5 cells/well or into 35-mm dishes at a density of 2×10^6 cells/well, cultured to 80% confluency in complete medium, then starved overnight in phenol red-free RPMI. Cells were then washed with fresh phenol red-free RPMI and treated. Cells were lysed in ice-cold lysis buffer consisting of 50 mM Tris (pH 6.8), 2% sodium dodecyl sulfate (SDS), and 10% glycerol. For analysis of PARP cleavage, medium was centrifuged at 1200 × *g* at 4 C to collect floating cells and adherent and floating cells were pooled and lysed. Lysates were heated for 5 min at 95 C and then sonicated for 10 sec on ice. After a 5-min centrifugation at 12,000 × *g*, supernatants were collected and protein concentrations determined. After addition of 50 mM dithiothreitol and 0.005% bromphenol blue, equal amounts of protein were subjected to SDS gel electrophoresis and blotted onto nitrocellulose membranes. Blots were blocked 1 h in blocking buffer [5% nonfat dry milk dissolved in 10 mM Tris-HCl (pH 7.4), 200 mM NaCl, and 0.1% Tween 20 (TBS-T)]. Blocked nitrocellulose blots were incubated overnight with primary antibody in 5% BSA and TBS-T, washed in TBS-T, then incubated 1 h with a 1:5000 dilution of the appropriate secondary antibody coupled with horseradish peroxidase in blocking

buffer. After washing, the immune complexes were detected by enhanced chemiluminescence (ECL) using Supersignal7 Ultra chemiluminescent substrate. Signals were detected using the UVP Bioimaging System and LabWorks 4.0 Image Acquisition Software and signal intensity quantified with Bio-Rad Molecular Analyst software. The following dilutions of the primary antibodies were used: phospho-Akt, Akt, cyclin D1, phospho-p44/42 MAPK, p44/42 MAPK, phospho-JNK, JNK, phospho-BAD, phospho-FKHR, phospho-IRS-1, phospho-PDK1, phosphoGSK-3β, and GSK, phospho-IGF-IR, IGF-IR, phospho-Shc, and Shc, 1:1000; PARP, 1:2000; and tubulin, 1:10,000.

IRS-1 immunoprecipitation

Cells were grown to 80% confluency, starved overnight, treated with vehicle or SPE for 6 h, and then treated with vehicle or 50 nM IGF-I for 10 min. Cells were then washed twice with ice-cold PBS and lysed in Nonidet P-40 lysis buffer [1% Ipegal, 150 mM NaCl, 10% glycerol, 20 mM Tris-Cl (pH 8), 1 mM EDTA, and 0.2% SDS]. Lysates were incubated on ice for 20 min with occasional inversion, and then centrifuged at 13,000 × *g* for 15 min at 4 C. The supernatant was transferred to a new tube and protein concentration determined. For immunoprecipitation, 500 μg of lysate were incubated with 5 μl of rabbit polyclonal anti-IRS-1 overnight at 4 C with rocking. The lysate was then incubated with 25 μl of protein-A-agarose beads for 2 h. Before loading onto 7.5% polyacrylamide gels, the beads were washed three times with lysis buffer and boiled in 25 μl 2× SDS sample buffer. After SDS gel electrophoresis, gels were blotted onto nitrocellulose membranes and blocked in blocking buffer for 1 h. Blots were incubated overnight with mouse monoclonal phosphotyrosine 20 (1:1000) in 5% BSA and TBS-T, washed in TBS-T, then incubated 1 h with a 1:5000 secondary antibody coupled with horseradish peroxidase in blocking buffer. Stripped blots were analyzed for levels of total IRS by incubating overnight with a 1:5000 dilution of rabbit polyclonal anti-IRS-1.

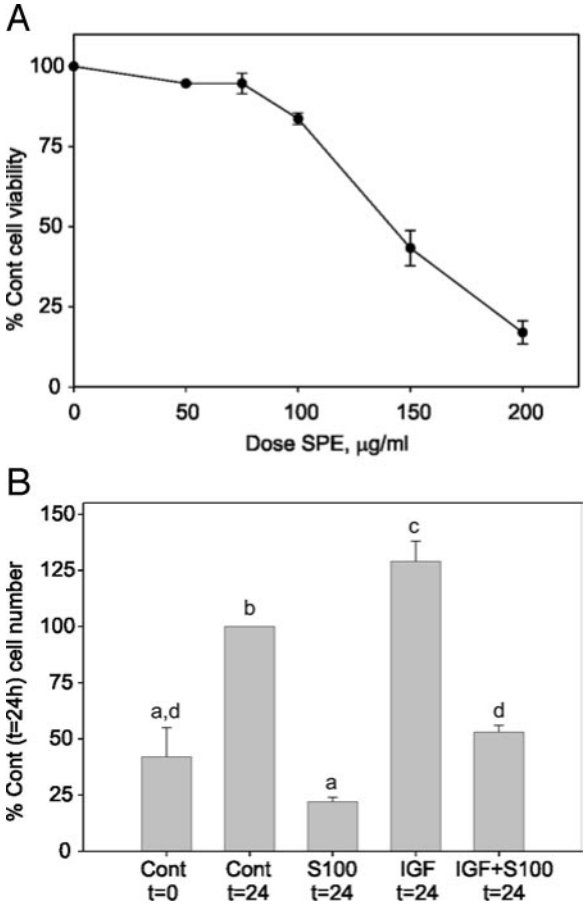

FIG. 1. SPE decreases cell P69 cell viability and proliferation. A, Cells were plated in six-well flasks, at a density of 4×10^5 cells/well, cultured in complete medium to 80% confluency, and then treated with varying doses of SPE for 24 h. Cell viability was determined by the MTS assay, as described in *Materials and Methods*. B, Effects of SPE on IGF-I-induced cell proliferation: P69 cells were plated in six-well flasks at a density of 2×10^5 cells/well, cultured in complete medium to 50% confluency, and then counted (Cont t = 0 h) or treated for 24 h with vehicle, 100 μg/ml SPE, 50 nM IGF-I or 100 μg/ml SPE plus 50 nM IGF-I, then counted (Cont t = 24 h, S100 t = 24 h, IGF t = 24 h, IGF + S100 t = 24 h). Data are expressed as the percentage of cells in the control treatment at 24 h. *Bars* ± SE, n = 3. Means with *different letters* are significantly different, $P < 0.05$.

Akt activity

Cells were plated into 35-mm dishes at a density of 2×10^6 cells/well, cultured to 80% confluency in complete medium, then starved overnight in phenol red-free RPMI. Cells were then washed with fresh phenol red-free RPMI and treated. Akt kinase activity was analyzed using a nonradioactive immunoprecipitation-kinase assay kit and measuring phosphorylation of GSK-3 by Western blot analysis as per manufacturer's instructions. Equal amounts of protein were immunoprecipitated, and the entire amount of immunoprecipitate was used in the subsequent kinase assay step.

Cell viability and cell proliferation assays

To test the effects of SPE on cell viability, cells were plated in six-well flasks at a density of 4×10^5 cells/well, cultured in complete medium to 80% confluency, starved overnight in phenol red-free RPMI, then treated with SPE for 24 h. Cell proliferation was determined by measuring the bioreduction of carboxymethylphenyl-2-(4-sulfophenyl)-2H-tetrazolium, inner salt (MTS) using the CellTiter 96 Aq_{ueous} Nonradioactive Cell Proliferation assay as per manufacturer's instructions. To measure the effects of SPE and IGF-I on cell proliferation, cells were plated in six-well flasks at a density of 2×10^5 cells/well, cultured in complete medium to 50% confluency, washed with PBS, then treated with vehicle or SPE in the presence or absence of IGF for 24 h. A hemocytometer was used to determine total cell counts before and after treatment.

Statistics

Data were analyzed with Sigma Stat 3.0 software (SPSS Science, Chicago, IL) using one-way ANOVA followed by a Fisher least significant difference test.

Results

SPE decreases P69 cell viability and inhibits cell proliferation

MTS assays were used to determine the effects of a 24-h SPE treatment on the viability of P69 cells that were 80%

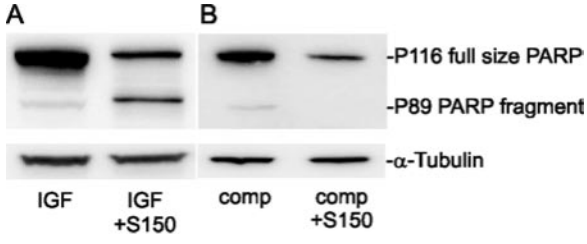

FIG. 2. SPE induces apoptosis in P-69 cells. Cell lysates (30 μg/lane) were analyzed for Caspase-3-mediated PARP cleavage activity by Western blot analysis using an anti-PARP antibody as described in *Materials and Methods*. A, A representative Western blot image is shown for 80% confluent, starved cells treated for 24 h with 50 nM IGF-I (IGF) or 50 nM IGF-I plus 150 μg/ml SPE (IGF + S150). B, A representative Western blot image is shown for starved, 80% confluent cells treated for 24 h with complete medium (comp) or complete medium containing 150 μg/ml SPE (comp + S150).

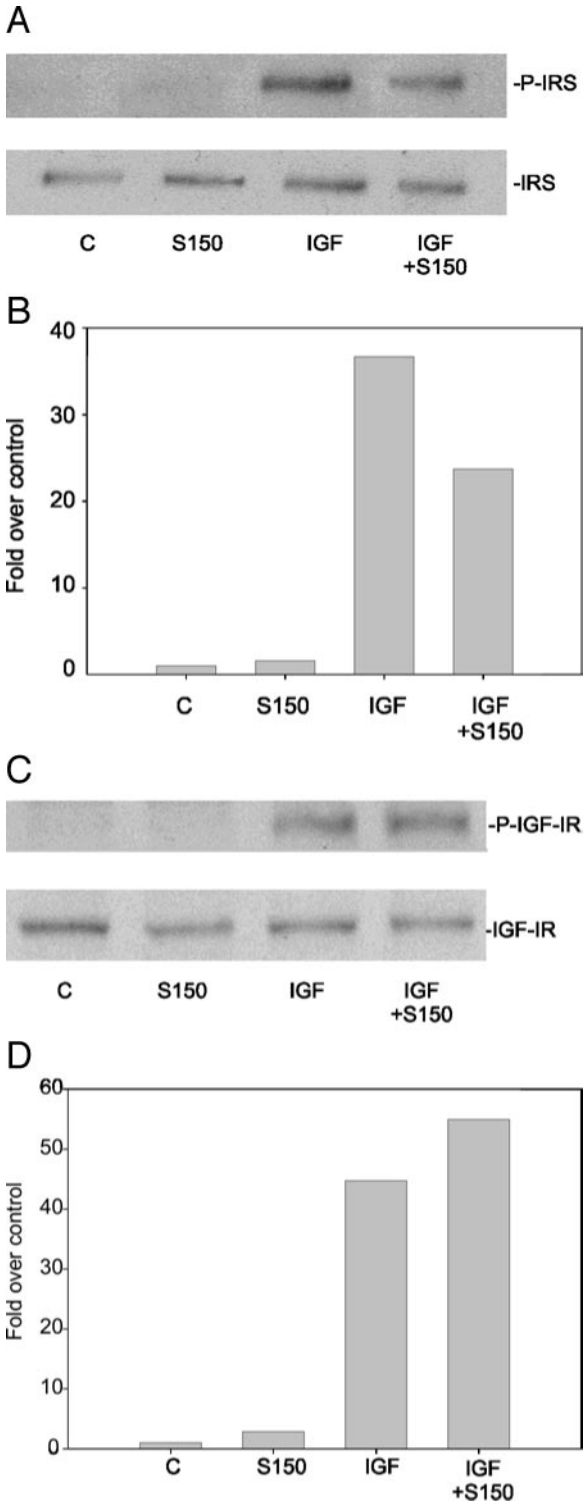

FIG. 3. SPE inhibits IGF-I-induced phosphorylation of IRS-1 but has no effect on IGF-I-induced IGF-IR phosphorylation. A, Immunoprecipitation was used to examine the effect of SPE on IGF-I-induced tyrosine phosphorylation of IRS-1 as described in *Materials and Methods*. A representative Western blot is shown in panel A for 80% confluent cells that were starved overnight, then treated for 6 h with vehicle or 150 μg/ml SPE (C, S150), or starved overnight, treated for 6 h with vehicle or 150 μg/ml SPE, then treated with 50 nM IGF-I for 10 min (IGF, S150 + IGF). The graph in panel B shows relative levels of phospho-IRS-1 normalized to total IRS-1 for cells that were treated as described in panel A, n = 2. C, Cell lysates were assayed for levels of phospho-IGF-IR and total IGF-IR by Western blot. A representative image is shown for cells that were treated as described in panel A. D, The graph shows relative levels of phospho-IGF-IR normalized to total IGF-IR for the same treatments described above, n = 2.

confluent at the time of treatment. The IC_{50} for inhibition of cell viability at 24 h was approximately 140 μg/ml (Fig. 1A). To test whether this treatment inhibited IGF-I-induced P69 cell proliferation, we treated cells at 50% confluency with vehicle, 100 μg/ml SPE, 50 nM IGF-I, or 100 μg/ml SPE plus 50 nM IGF-I, and assessed proliferation by counting cells. IGF-I induced a 29% increase in the number of cells when compared with control, and 100 μg/ml SPE inhibited both basal and IGF-I-induced proliferation (Fig. 1B).

SPE induces apoptosis in P69 cells

To determine whether SPE induced apoptosis in P69 cells, we used Western blot analysis to monitor the cleavage of the enzyme PARP, a target for caspase-3 (31). As shown in the representative Western blot in Fig. 2A, treatment of starved cells with 50 nM IGF-I plus 150 μg/ml SPE for 24 h caused the disappearance of 116-kDa, full-size PARP, and a concomitant accumulation of its 89-kDa cleavage product when compared with starved cells treated with IGF-I alone. Treatment of 80%-confluent P69 cells with 150 μg/ml SPE in complete media resulted in the disappearance of 116-kDa, full-size PARP (and the appearance of low-molecular-weight cleavage products, data not shown) when compared with control.

SPE inhibits IGF-I-induced phosphorylation of IRS-1

Selective immunoprecipitation of IRS-1 from cell lysates, followed by Western blot analysis of phosphorylated tyrosine residues, suggests that SPE inhibits IGF-I-induced phosphorylation of IRS-1 (Fig. 3, A and B; n = 2). Cell lysates were assayed for the effects of SPE on IGF-I-induced phosphorylation of IGF-IR; a representative Western blot is shown in Fig. 3C. As shown in the graph in Fig. 3D, which represents duplicate treatments, SPE had no apparent effect on IGF-I-induced phosphorylation of IGF-IR. SPE also had no effect on the modest activation of Shc that was induced by IGF-I; neither IGF-I nor SPE had an effect on the serine phosphorylation of PDK1 (data not shown).

SPE decreases IGF-I-induced activation of Akt but not ERK

Cell lysates were assayed for levels of phospho-Akt, total Akt, and tubulin by Western blot analysis. A representative Western blot is shown in Fig. 4A. As shown in the graph in Fig. 4B, treatment of starved cells with 50 nM IGF-I for 10 min resulted in a 34-fold increase in levels of phosphorylated Akt^{ser473} when normalized to Akt and α-tubulin when compared with control. IGF-I-induced Akt phosphorylation was reduced 52% by a 6-h pretreatment with 150 μg/ml SPE. Similar results were obtained with an antiphosphothreonine 308 antibody (results not shown). Akt kinase activity, analyzed by an *in vitro* kinase assay after immunoprecipitation of Akt from cell lysates, suggested a decrease in IGF-I-

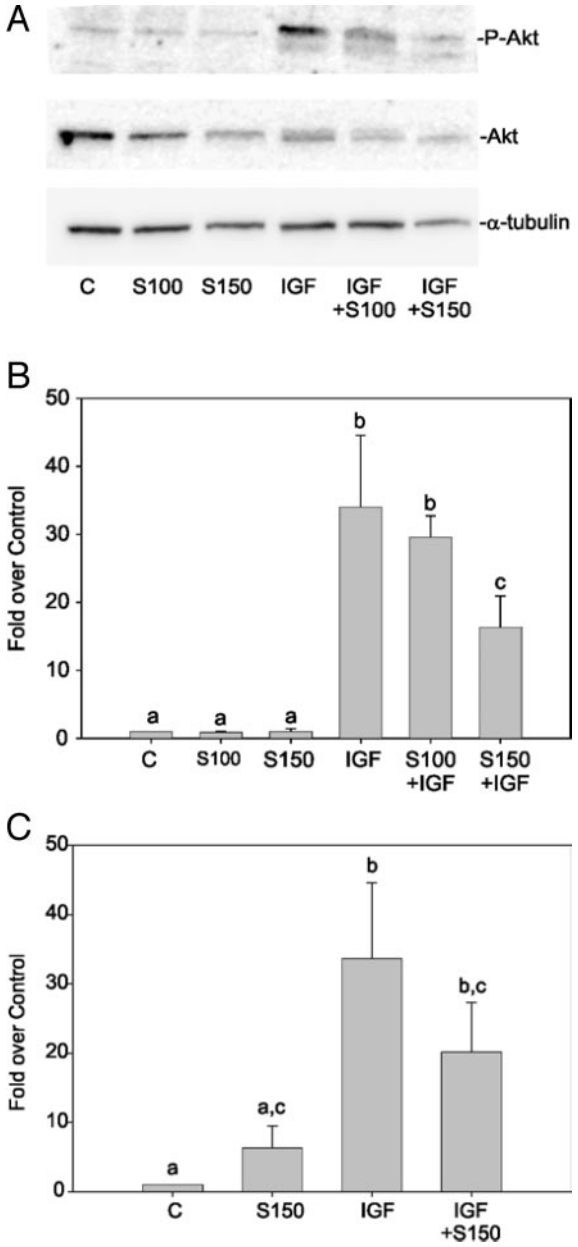

FIG. 4. SPE decreases IGF-I-induced phosphorylation and activation of Akt. A, Cell lysates (30 μg/lane) were assayed for levels of phopho-Akt, Akt and α-tubulin by Western blot analysis as described in *Materials and Methods*. A representative image is shown for 80% confluent cells that were starved overnight, then treated for 6 h with vehicle, 100 μg/ml SPE or 150 μg/ml SPE (C, S100, S150), or starved overnight, pretreated for 6 h with vehicle, 100 μg/ml SPE or 150 μg/ml SPE, then treated with 50 nM IGF for 10 min (IGF, IGF + S100, IGF + S150). B, The graph shows relative levels of phospho-Akt normalized to Akt and α-tubulin for cells treated as described in panel A. *Bars* $\pm$ SE, n = 5. Means with *different letters* are significantly different, $P < 0.05$. C, Akt kinase activity was determined by an immunoprecipitation kinase assay as described in *Materials and Methods*. The graph shows relative levels of phosphorylated GSK-3 for cells that were treated as described in the legend to Fig. 3A. *Bars* $\pm$ SE, n = 5. Means with *different letters* are significantly different, $P < 0.05$.

induced phosphorylation of the Akt substrate GSK-3β (Fig. 4C).

Cell lysates were analyzed for levels of phosphorylated and total ERK1/2 by Western blot analysis, a representative blot is shown in Fig. 5A. As shown in Fig. 5B, SPE at a dose of 150 μg/ml increased MAPK phosphorylation 30-fold when normalized to total MAPK and α-tubulin. Treatment with IGF-I increased MAPK phosphorylation 50-fold and IGF-I-induced phosphorylation was not affected by SPE.

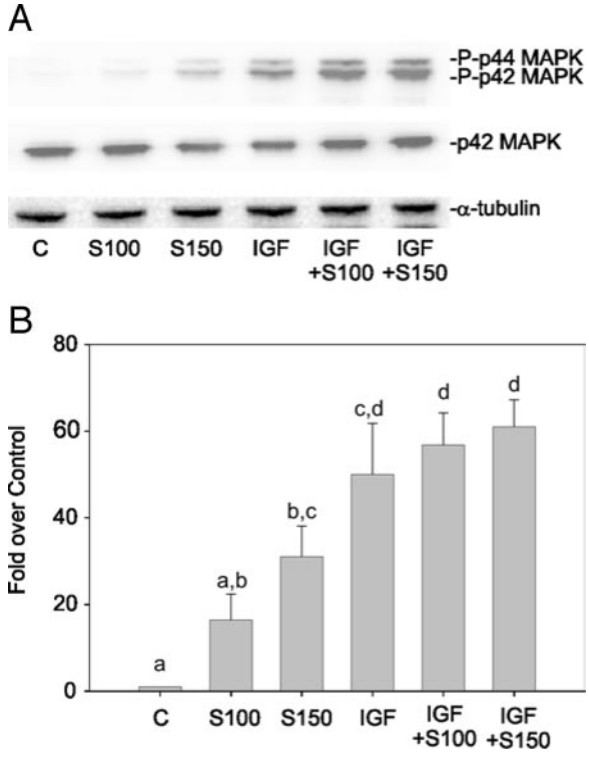

FIG. 5. SPE alone induces phosphorylation of p44/42 MAPK but does not affect IGF-I-induced phosphorylation of p44/42 MAPK. A, Cell lysates (30 μg/lane) were assayed for levels of phopho-MAPK, total MAPK and α-tubulin by Western blot analysis as described in *Materials and Methods*. A representative image is shown for cells treated as described in the legend to Fig. 4A. B, The graph shows relative levels of phopho-MAPK normalized to MAPK and α-tubulin for cells treated as described above. *Bars* $\pm$ SE, n = 4. Means with *different letters* are significantly different, $P < 0.05$.

SPE decreases phosphorylation of specific downstream components of the PI3K/Akt signaling pathway

We next sought to determine whether SPE had effects on downstream components of the PI3K/Akt signaling pathway. $p70^{S6K}$ phosphorylation (Ser 421)/(Thr 424) and total $p70^{S6K}$ expression were detected using Western blot analysis, and a representative blot is shown in Fig. 6A. As shown in Fig. 6B, a 10-min treatment with IGF-I caused a 2.8-fold increase in the levels of phosphorylated $p70^{S6K}$ when normalized to total $p70^{S6K}$ and α-tubulin. Pretreatment with 150 μg/ml SPE returned levels of phospho-$p70^{S6K}$ to that of controls. We next tested the effects of SPE on IGF-I-induced phosphorylation of the endogenous Akt substrate GSK-3β. A representative blot is shown in Fig. 6C. Treatment of starved cells with IGF-I caused a 6-fold increase in the levels of phosphorylated GSK-3β when normalized to total GSK-3β and α-tubulin, and pretreatment with 150 μg/ml SPE decreased IGF-I-mediated GSK-3β phosphorylation (Fig. 6D).

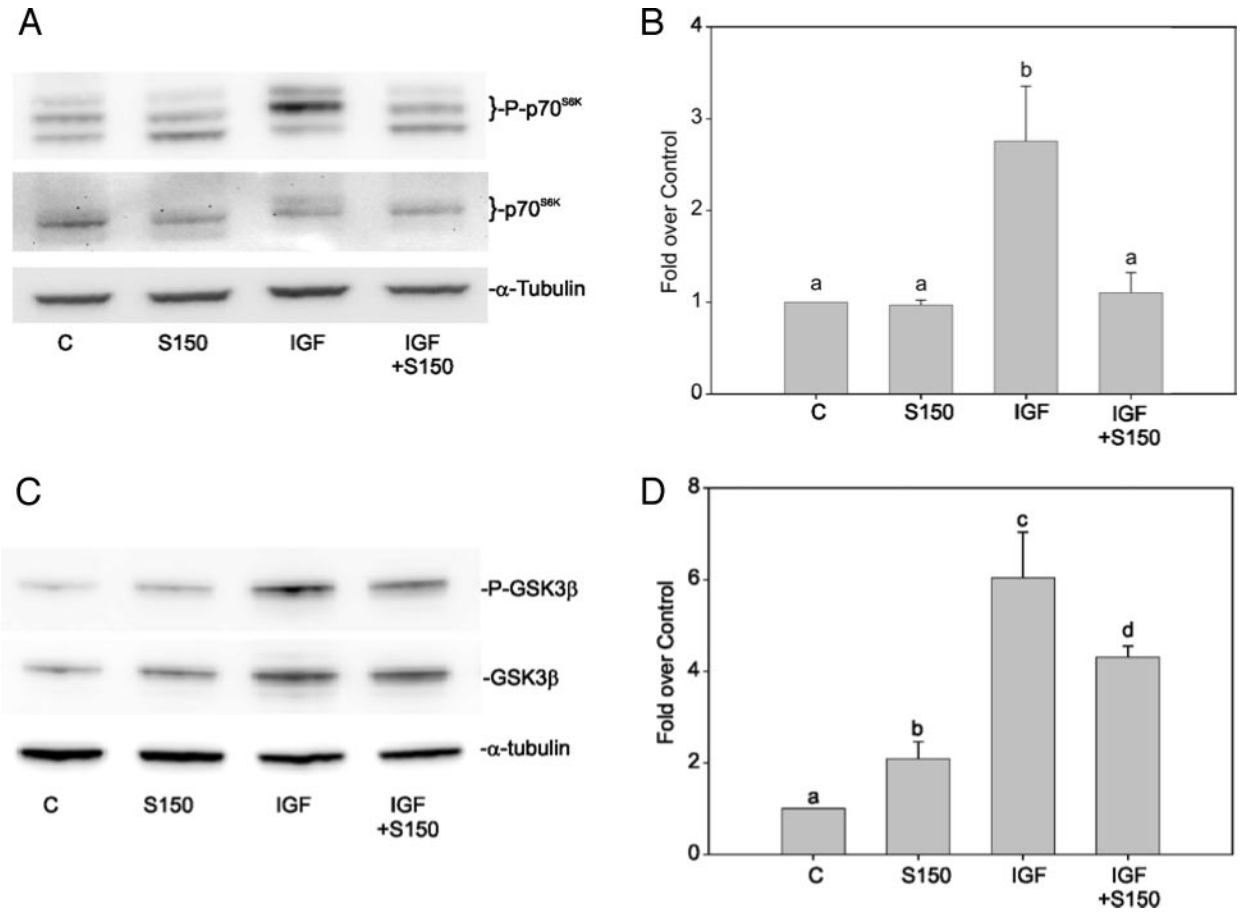

FIG. 6. SPE decreases IGF-I-induced phosphorylation of $p70^{S6K}$ and GSK3β. A, Cell lysates (30 μg/lane) were assayed for levels of phospho-$p70^{S6K}$ (Thr 421/Ser 424), total $p70^{S6K}$, and α-tubulin by Western blot analysis as described in *Materials and Methods*. A representative image is shown cells treated as described in the legend to Fig. 3A. B, Relative levels of phopho-$p70^{S6K}$ normalized to total $p70^{S6K}$ and α-tubulin for cells treated as described above. *Bars* ± SE, n = 3. Means with *different letters* are significantly different, $P < 0.05$. C, Cell lysates (30 μg/lane) were assayed for levels of phopho-GSK3β, GSK3β and α-tubulin by Western blot analysis as described in *Materials and Methods*. A representative image is shown for cells treated as described in the legend to Fig. 3A. D, Relative levels of phospho-GSK3β normalized to total GSK3β and α-tubulin for cells treated as described above. *Bars* ± SE, n = 3. Means with *different letters* are significantly different, $P < 0.05$.

A representative Western blot illustrating the effects of SPE on cyclin D1 protein levels is shown in Fig. 7A. As shown in Fig. 7B, a 6-h treatment of starved cells with 50 nM IGF-I increased cyclin D1 levels by 70%. Treatment with SPE at a dose of 150 μg/ml reduced cyclin D1 to control levels. SPE had no effect on levels of IGF-I-induced phosphorylation of $FKHR^{Ser256}$; phophorylated Bad^{Ser136} was not detectable in IGF-I-treated P69 cells by Western blot analysis (data not shown).

SPE increases JNK phosphorylation

As shown in Fig. 8, a 6-h treatment of starved cells with SPE at doses of 100 μg/ml and 150 μg/ml increased phosphorylation of JNK by 6-fold, and SPE-induced JNK phosphorylation was unaffected by cotreatment with IGF-I.

Discussion

This study supports the hypothesis that SPE acts, in part, to suppress IGF-I signaling in the P69 prostate epithelial cell line. Previous *in vitro* studies have demonstrated multiple potential mechanisms of action of SPE, including inhibition of 5α-reductase, adrenergic receptor blockade, inhibition of fibroblast growth factor-induced prostate proliferation, inhibition of DHT binding to the AR, and inhibition of cyclooxygenase, lipoxygenase, and Bcl-2 (23). Here we demonstrate for the first time that SPE has inhibitory effects on the PI3K/Akt signaling pathway and activating effects on the proapoptotic enzyme SAPK/JNK. These effects indicate additional mechanisms by which SPE could mitigate the urological symptoms associated with BPH.

We chose the P69 prostate epithelial cell line as a model because this immortalized cell line is poorly tumorigenic and nonmetastatic and expresses levels of IGF-IR similar to those seen in primary prostate epithelial cells (30). Whereas the increase in prostate volume in BPH is predominantly caused by increased cellular hyperplasia and reduced apoptosis in the stroma, we consider P69 cells a relevant *in vitro* model for studying the effects of SPE on BPH because IGF-I acts as an important paracrine growth factor in prostate epithelium, its effects are mediated through the IGF-IR, and BPH is accompanied by epithelial growth (2, 32, 33). Because prostate cancer (CaP) develops from glandular epithelial cells (34),

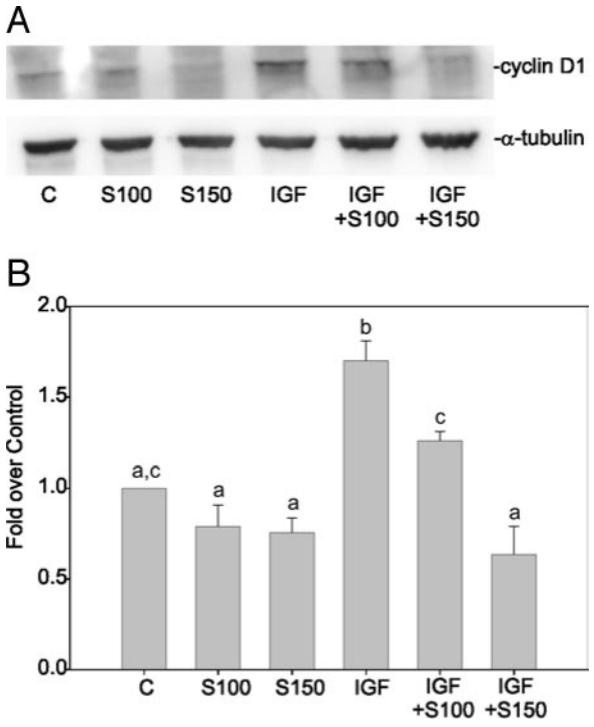

FIG. 7. SPE decreases IGF-I-mediated increase in cyclin D1. A, Cell lysates (30 μg/lane) were assayed for levels of cyclin D1 and tubulin by Western blot analysis as described in *Materials and Methods*. A representative image is shown for cells that were treated as described in the legend to Fig. 4A. B, Relative levels of cyclin D1 normalized to α-tubulin for cells treated as described above. *Bars* ± SE, n = 3. Means with *different letters* are significantly different, $P < 0.05$.

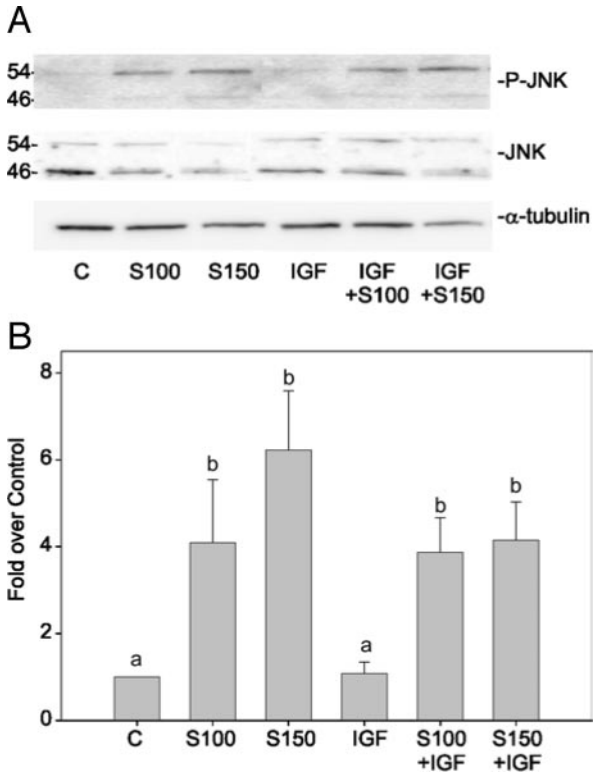

FIG. 8. SPE increases JNK phosphorylation and SPE-induced phosphorylation is unaffected by the additional presence of IGF-I. Cell lysates were assayed for levels of phospho-JNK, total JNK, and tubulin by Western blot. A, A representative image is shown for cells treated as described in the legend to Fig. 4A. B, The graph shows relative levels of phospho-JNK normalized to total JNK and α-tubulin for the same treatments described above. *Bars* ± SE, n = 3. Means with *different letters* are significantly different, $P < 0.05$.

P69 cells can also be used in the future to determine whether SPE exerts chemopreventive properties against the development of CaP.

The IC_{50} for inhibition of P69 cell viability by SPE at 24 h was approximately 140 μg/ml, slightly higher than the IC_{50} of 100 μg/ml reported by Iguchi *et al.* (27) for LNCaP cells, but consistent with the fact that P69 cells do not express AR. Studies comparing the effects of SPE on prostate cancer cell lines show that SPE is more toxic to the hormone-dependent LNCaP cell line than PC3 cells (which do not express detectable levels of AR), a phenomenon that probably reflects the antiandrogenic actions of SPE (35). The recommended dose of SPE is 320 mg/d. Pharmacokinetic studies in humans show that a single 640-mg dose of SPE leads to peak plasma levels of 2.6 μg/ml (36). Because SPE is a self-prescribed herbal supplement, dose and duration of treatment could be extremely variable. In addition, reports suggest the specificity of SPE for prostate tissue. Oral administration of SPE supplemented with ^{14}C-labeled oleic and lauric acids to rats demonstrate that radioactivity is selectively concentrated in the prostate (37). SPE selectively and specifically induces apoptosis in human primary epithelial and stromal cells of prostate origin, but not other target organs (38). Thus, although the concentrations of SPE used to treat P69 cells *in vitro* are relatively high in comparison to peak plasma levels after a single dose, they are relevant, given the possibilities for variability in dose and for tissue-specific accumulation with prolonged treatment.

To test the specificity of SPE on IGF-I-induced cell proliferation, we treated P69 cells with SPE in the presence or absence of IGF-I for 24 h. Cells were treated at 50% confluency to detect the proliferative effects of IGF-I. SPE at a dose of 100 μg/ml blocked both basal and IGF-I-induced cell proliferation. Exponentially growing P69 cells appeared to be inherently more susceptible to SPE-induced toxicity than confluent cells, which is in agreement with studies by Garzotto *et al.* (39), who reported that LNCaP cells in plateau-phase (a condition that more closely resembles the state of cells *in vivo*) are more resistant to apoptosis than cells undergoing exponential growth. Treatment of 80% confluent P69 cells with SPE at a dose of 150 μg/ml for 24 h triggered apoptotic cell death (as assayed by PARP cleavage) either when cells were stimulated with IGF-I or grown in complete media. Similarly, treatment with 120 μg/ml SPE for 24 h has been shown to induce cell death in the LNCaP prostate cancer cell line, with nuclear morphology exhibiting both apoptotic and necrotic features (27). Our results, which demonstrate that SPE induces apoptotic cell death and inhibits cell proliferation in the presence of IGF-I, suggest that SPE specifically counteracts some of the *in vitro* proliferative and antiapoptotic effects of IGF-I.

To begin to understand the mechanism by which SPE inhibits IGF-I-induced cell proliferation and protection from

apoptosis, we analyzed the effects of SPE on the PI3K/Akt and MAPK pathways, the two major signaling pathways activated by binding of IGF-I to the IGF-IR. Pretreatment with SPE for 6 h decreased IGF-I-induced Akt phosphorylation and Akt kinase activity and decreased IGF-I-induced phosphorylation of the PI3K/Akt substrates GSK-3β and $p70^{S6K}$. Treatment with SPE alone, at a dose of 150 μg/ml, increased levels of phosphorylated ERK, but had no effect on IGF-I-induced ERK phosphorylation. Because previous studies have suggested that PI3K/Akt/ $p70^{S6K}$ activation is necessary for the induction of cyclin D1 and cell cycle progression in prostate cells (40), we tested whether IGF-I-induced cyclin D1 levels were altered by SPE. SPE at a dose of 150 μg/ml reduced cyclin D1 levels to that of starved cells. We next tested the effects of SPE on upstream components of the PI3K/Akt pathway. SPE had no effect on levels of IGF-IR phosphorylation; however, IGF-I-induced tyrosine phosphorylation of the adapter protein IRS-1, which couples the activated IGF-IR to the p85 regulatory subunit of PI3K, was inhibited by 32%. Neither IGF-I nor SPE had an effect on $PDK1^{ser241}$ phosphorylation, which is in agreement with results seen in other cell lines, where Ser 241 is phosphorylated under basal conditions and is refractory to additional phosphorylation upon IGF-I stimulation (41). Taken together, our results suggest that SPE exerts direct effects on specific components of the IGF-I signaling pathway. It is likely that SPE affects IGF-I signaling at a single point, and inhibition of downstream signaling is a result of this single event. IRS-1 is the uppermost signaling molecule in which we see effects of SPE on IGF-I-induced phosphorylation. Because IRS-1 couples the active IGF-IR to both the PI3K/Akt and MAPK pathways, we would have initially predicted that there would be effects on downstream components of both pathways. The independent increase in ERK phosphorylation induced by SPE in the absence of IGF-I may abrogate downstream inhibitory effects of SPE on IGF-I-induced phosphorylation of IRS-1, resulting in no net change in IGF-I-induced ERK phosphorylation. Alternatively, specific residues linking IRS-1 to MAPK *vs.* PI3K may be differentially inhibited by SPE. Previous studies report selective effects of lipid mediators on the PI3K/Akt and MAPK pathways. Sphingosine-1-phosphate, which inhibits IGF-I-induced human epidermal keratinocyte proliferation, independently activates the ERK pathway while inactivating IGF-I-induced activation of Akt (42). C2-ceramide inhibits NGF-induced activation of Akt in PC12 cells, while increasing levels of NGF-induced MAPK phosphorylation (43). In addition, black tea phenols, which reduce IGF-I-induced phosphorylation of the IGF-IR, phosphorylation of Akt and phosphorylation of GSK-3β, have no effect on the constitutively high MAPK phosphorylation seen in DU-145 cells (44). Recent reports also suggest that epigallocatechin-3-gallate and theaflavins, the major polyphenols in green and black tea, decrease levels of PI3K and phospho-Akt and increase ERK1/2 phosphorylation in LNCaP cells and DU-145 cells (45). Selective inhibition of IGF-I-induced activation of the PI3K/Akt pathway may be an important mechanism by which SPE inhibits cell proliferation and induces apoptosis in P69 cells.

In our effort to further characterize the mechanism by which SPE induces apoptosis in P69 cells, we tested the effects of SPE on the SAPK/JNK signaling pathway, which has been mechanistically implicated in the initiation of apoptosis in many cell types (46). We demonstrated that SPE treatment resulted in a 5- to 6-fold increase in levels of phosphorylated SAPK/JNK, and this increase was unaffected by the additional presence of IGF-I. SAPK/JNK activation has been correlated with the phosphorylation and inactivation of the proto-oncogene Bcl-2, and studies have demonstrated that SPE-induced apoptosis in LNCaP cells is associated with decreased expression of Bcl-2 (26, 47). The SAPK/JNK pathway has been shown to attenuate IGF-I responses in breast cancer cells by enhancing IRS-1 Ser 312 phosphorylation (17). Further experimental work will address the mechanism by which SPE induces SAPK/JNK phosphorylation and whether it is involved in inhibition of Bcl-2 expression and/or enhanced phosphorylation of IRS-1 Ser 312 in P69 cells.

SPE is a complex mixture composed of 93.5% saturated and unsaturated fatty acids that are present in both the free and esterified forms (with a high content of medium-chain fatty acids such as lauric acid, myristic acid, palmitic acid, and oleic acid), as well as small amounts of phytosterols and flavonoids (www.indena.com). As such, it is likely that its components could exert pleiotropic and synergistic effects. A potential mechanism by which SPE exerts AR-independent effects on IGF-I signaling and apoptosis is via fatty acid-induced increases in the sphingolipid ceramide. Ceramide-induced apoptosis and suppression of cell growth involves activation of SAPK/JNK as well as activation of protein phosphatase 2A, resulting in the dephosphorylation and inactivation of Akt (48–50). Fatty acid-induced elevations in ceramide inhibit insulin-stimulated phosphorylation of Akt and GSK in skeletal muscle cells and induce apoptosis in pancreatic β-cells (51, 52). Ceramide can be synthesized by catabolism of membrane bound sphingomyelin or via the *de novo* condensation of sphinganine and fatty acyl-coenzyme A by the enzyme ceramide synthase. The mycotoxin FB_1 inhibits the *de novo* pathway. Future studies will determine whether SPE treatment increases ceramide levels in P69 cells. In preliminary studies, FB_1 did not effect SPE-induced inhibition of proliferation, apoptosis, or PI3K/Akt signaling in P69 cells, suggesting that, if involved, ceramide is most likely derived from sphingomyelin.

SPE is the most widely used, self-prescribed treatment for BPH, and recent reports document widespread use of SPE in conjunction with conventional medical treatments by men diagnosed with CaP (53). Accumulating evidence suggests that dysregulation of the IGF-I system is involved in the pathogenesis of human BPH and in the initiation and progression of CaP (2, 32, 54–56). Finasteride, a conventionally prescribed pharmaceutical treatment for BPH, has been shown to suppress IGF-I and IGF-IR gene expression, inhibit Akt and MAPK activation, and induce apoptosis *in vivo* (57–60). Studies also suggest that the effectiveness of vitamin D_3 analogs in the treatment of BPH are, in part, due to their ability to inhibit the mitogenic activity of IGF-I in BPH cells (54, 61). Akt activation in transgenic mice in which the expression of activated Akt is spatially restricted to the prostate leads to $p70^{s6k}$ activation and prostatic intraeptithelial neoplasia (62). Several *in vitro* studies show that SPE inhibits the

growth of prostate cancer cell lines in culture, suggesting that it may possess chemopreventative potential (26, 27, 35). Our results support the hypothesis that SPE may counteract the *in vitro* proliferative and antiapoptotic effects of IGF-I by inhibiting specific components of the IGF-I-induced signaling pathway, including Akt and $p70^{s6k}$. In addition, SPE induces phosphorylation of the intracellular signaling enzyme SAPK/JNK, a negative regulator of IGF-I signaling and a key promoter of apoptosis. Although caution must be exercised when attributing the actions of pharmacological agents on cells in culture to effects observed *in vivo*, our results, in conjunction with previous studies (26, 27, 53), help explain the efficacy of SPE in the treatment of BPH symptoms and support the need for future studies that evaluate the use of SPE as an alternative chemopreventative agent for CaP.

Acknowledgments

Received December 18, 2003. Accepted March 10, 2004.

Address all correspondence and requests for reprints to: Dr. Charles E. Roselli, Department of Physiology and Pharmacology L334, Oregon Health and Science University, 3181 Sam Jackson Park Road, Portland, Oregon 97239. E-mail: rosellic@ohsu.edu.

This work was supported by National Institutes of Health Grant R21 AT000670 (to C.E.R.), Department of Defense Prostate Cancer Research Program Grant PC10273 and the Lematta Foundation of Southwest Washington (to C.T.R.) and Reproductive Biology Training Grant T32 HD07133 from the National Institute of Child Health and Human Development (to T.L.W.).

References

1. **Jacobsen SJ, Girman CJ, Lieber MM** 2001 Natural history of benign prostatic hyperplasia. Urology 58:5–16
2. **Culig Z, Hobisch A, Cronauer MV, Radmayr C, Hittmair A, Zhang J, Thurnher M, Bartsch G, Klocker H** 1996 Regulation of prostatic growth and function by peptide growth factors. Prostate 28:392–405
3. **Peehl DM, Cohen P, Rosenfeld RG** 1995 The insulin-like growth-factor system in the Prostate. World J Urol 13:306–311
4. **Cohen P, Peehl DM, Baker B, Liu F, Hintz RL, Rosenfeld RG** 1994 Insulin-like growth-factor axis abnormalities in prostatic stromal cells from patients with benign prostatic hyperplasia. J Clin Endocrinol Metab 79:1410–1415
5. **Dong GY, Rajah R, Vu T, Hoffman AR, Rosenfeld RG, Roberts CT, Peehl DM, Cohen P** 1997 Decreased expression of Wilms' tumor gene WT-1 and elevated expression of insulin growth factor-II (IGF-II) and type 1 IGF receptor genes in prostatic stromal cells from patients with benign prostatic hyperplasia. J Clin Endocrinol Metab 82:2198–2203
6. **LeRoith D, Roberts CT** 2003 The insulin-like growth factor system and cancer. Cancer Lett 195:127–137
7. **Adams TE, Epa VC, Garrett TPJ, Ward CW** 2000 Structure and function of the type 1 insulin-like growth factor receptor. Cell Mol Life Sci 57:1050–1093
8. **Vivanco I, Sawyers CL** 2002 The phosphatidylinositol 3-kinase-AKT pathway in human cancer. Nat Rev Cancer 2:489–501
9. **Ghosh PM, Bedolla R, Mikhailova M, Kreisberg JI** 2002 RhoA-dependent murine prostate cancer cell proliferation and apoptosis: role of protein kinase Cζ. Cancer Res 62:2630–2636
10. **Diehl JA, Cheng MG, Roussel MF, Sherr CJ** 1998 Glycogen synthase kinase 3 β regulates cyclin D1 proteolysis and subcellular localization. Genes Dev 12:3499–3511
11. **Muise-Helmericks RC, Grimes HL, Bellacosa A, Malstrom SE, Tsichlis PN, Rosen N** 1998 Cyclin D expression is controlled post-transcriptionally via a phosphatidylinositol 3-kinase Akt-dependent pathway. J Biol Chem 273:29864–29872
12. **Kandel ES, Hay N** 1999 The regulation and activities of the multifunctional serine/threonine kinase Akt/PKB. Exp Cell Res 253:210–229
13. **Grammer TC, Cheatham L, Chou MM, Blenis J** 1996 The p70(S6K) signalling pathway: a novel signalling system involved in growth regulation. Cancer Surv 27:271–292
14. **Harada H, Andersen JS, Mann M, Terada N, Korsmeyer SJ** 2001 p70S6 kinase signals cell survival as well as growth, inactivating the pro-apoptotic molecule BAD. Proc Natl Acad Sci USA 98:9666–9670
15. **Chen YR, Meyer CF, Tan TH** 1996 Persistent activation of c-Jun N-terminal kinase 1 (JNK1) in γ radiation-induced apoptosis. J Biol Chem 271:631–634
16. **Wang TH, Wang HS, Ichijo H, Giannakakou P, Foster JS, Fojo T, Wimalasena J** 1998 Microtubule-interfering agents activate c-Jun N-terminal kinase stress-activated protein kinase through both ras and apoptosis signal-regulating kinase pathways. J Biol Chem 273:4928–4936
17. **Mamay CL, Mingo-Sion AM, Wolf DM, Molina MD, Van Den Berg CL** 2003 An inhibitory function for JNK in the regulation of IGF-I signaling in breast cancer. Oncogene 22:602–614
18. **Aguirre V, Werner ED, Giraud J, Lee YH, Shoelson SE, White MF** 2002 Phosphorylation of Ser(307) in insulin receptor substrate-1 blocks interactions with the insulin receptor and inhibits insulin action. J Biol Chem 277:1531–1537
19. **Aguirre V, Uchida T, Yenush L, Davis R, White MF** 2000 The c-Jun NH2-terminal kinase promotes insulin resistance during association with insulin receptor substrate-1 and phosphorylation of Ser(307). J Biol Chem 275:9047–9054
20. **Herrmann JL, Bruckheimer E, McDonnell TJ** 1996 Cell death signal transduction and Bcl-2 function. Biochem Soc Trans 24:1059–1065
21. **Steiner JF** 1996 Clinical pharmacokinetics and pharmacodynamics of finasteride. Clin Pharmacokin 30:16–27
22. **Lowe FC, Fagelman E** 2002 Phytotherapy in the treatment of benign prostatic hyperplasia. Curr Opin Urol 12:15–18
23. **Gerber GS** 2000 Saw palmetto for the treatment of men with lower urinary tract symptoms. J Urol 163:1408–1412
24. **Wilt TJ, Ishani A, Rutks I, MacDonald R** 2000 Phytotherapy for benign prostatic hyperplasia. Public Health Nutr 3:459–472
25. **Koch E** 2001 Extracts from fruits of saw palmetto (*Sabal serrulata*) and roots of stinging nettle (*Urtica dioica*): viable alternatives in the medical treatment of benign prostatic hyperplasia and associated lower urinary tracts symptoms. Planta Med 67:489–500
26. **Goldmann WH, Sharma AL, Currier SJ, Johnston PD, Rana A, Sharma CP** 2001 Saw palmetto berry extract inhibits cell growth and Cox-2 expression in prostatic cancer cells. Cell Biol Int 25:1117–1124
27. **Iguchi K, Okumura N, Usui S, Sajiki H, Hirota K, Hirano K** 2001 Myristoleic acid, a cytotoxic component in the extract from serenoa repens, induces apoptosis and necrosis in human prostatic LNCaP cells. Prostate 47:59–65
28. **Vacherot F, Azzouz M, Gil-Diez-De-Medina S, Colombel M, de la TA, Lefrere Belda MA, Abbou CC, Raynaud JP, Chopin DK** 2000 Induction of apoptosis and inhibition of cell proliferation by the lipido-sterolic extract of Serenoa repens (LSESr, Permixon in benign prostatic hyperplasia. Prostate 45:259–266
29. **Bae VL, Jacksoncook CK, Brothman AR, Maygarden SJ, Ware JL** 1994 Tumorigenicity of Sv40 T-antigen immortalized human prostate epithelial-cells—association with decreased epidermal growth-factor receptor (Egfr) expression. Int J Cancer 58:721–729
30. **Bae VL, Jackson-Cook CK, Maygarden SJ, Plymate SR, Chen J, Ware JL** 1998 Metastatic sublines of an SV40 large T antigen immortalized human prostate epithelial cell line. Prostate 34:275–282
31. **Lazebnik YA, Kaufmann SH, Desnoyers S, Poirier GG, Earnshaw WC** 1994 Cleavage of poly(Adp-ribose) polymerase by A proteinase with properties like ice. Nature 371:346–347
32. **Marcelli M, Cunningham GR** 1999 Hormonal signaling in prostatic hyperplasia and neoplasia. J Clin Endocrinol Metab 84:3463–3468
33. **Cohen P, Peehl DM, Lamson G, Rosenfeld RG** 1991 Insulin-like growth-factors (Igfs), Igf receptors, and Igf-binding proteins in primary cultures of prostate epithelial-cells. J Clin Endocrinol Metab 73:401–407
34. **Hanahan D, Weinberg RA** 2000 The hallmarks of cancer. Cell 100:57–70
35. **Ravenna L, Di Silverio F, Russo MA, Salvatori L, Morgante E, Morrone S, Cardillo MR, Russo A, Frati L, Gulino A, Petrangeli E** 1996 Effects of the lipidosterolic extract of Serenoa repens (Permixon) on human prostatic cell lines. Prostate 29:219–230
36. **De Bernardi Di Valserra M, Tripode AS** 1994 Rectal bioavailability and pharmacokinetics in healthy volunteers of serenoa repens new formulation. Arch Med Intern 46:7–86
37. **Chevalier G, Benard P, Cousse H, Bengone T** 1997 Distribution study of radioactivity in rats after oral administration of the lipido/sterolic extract of Serenoa repens (Permixon(R)) supplemented with [1-C-14]-lauric acid, [1-C-14]-oleic acid or [4-C-14]-β-sitosterol. Eur J Drug Metab Pharmacokin 22:73–83
38. **Bayne CW, Ross M, Donnelly F, Habib FK** 2000 The selectivity and specificity of the actions of the lipido-sterolic extract of serenoa repens (Permixon (R)) on the prostate. J Urol 164:876–881
39. **Garzotto M, Haimovitz-Friedman A, Liao WC, White-Jones M, Huryk R, Heston WDW, Cardon-Cardo C, Kolesnick R, Fuks Z** 1999 Reversal of radiation resistance in LNCaP cells by targeting apoptosis through ceramide synthase. Cancer Res 59:5194–5201
40. **Gao N, Zhang Z, Jiang BH, Shi XL** 2003 Role of PI3K/AKT/mTOR signaling in the cell cycle progression of human prostate cancer. Biochem Biophys Res Commun 310:1124–1132
41. **Vanhaesebroeck B, Leevers SJ, Panayotou G, Waterfield MD** 1997 Phosphoinositide 3-kinases: a conserved family of signal transducers. Trends Biochem Sci 22:267–272
42. **Kim DS, Kim SY, Kleuser B, Schafer-Korting M, Kim KH, Park KC** 2004 Sphingosine-1-phosphate inhibits human keratinocyte proliferation via Akt/protein kinase B inactivation. Cell Signal 16:89–95
43. **Salinas M, Lopez-Valdaliso R, Martin D, Alvarez A, Cuadrado A** 2000 In-

hibition of PKB/Akt1 by C2-ceramide involves activation of ceramide-activated protein phosphatase in PC12 cells. Mol Cell Neurosci 15:156–169
44. **Klein RD, Fischer SM** 2002 Black tea polyphenols inhibit IGF-I-induced signaling through Akt in normal prostate epithelial cells and Du145 prostate carcinoma cells. Carcinogenesis 23:217–221
45. **Siddiqui IA, Adhami VM, Afaq F, Ahmad N, Mukhtar H** 2004 Modulation of phosphatidylinositol-3-kinase/protein kinase B- and mitogen-activated protein kinase-pathways by tea polyphenols in human prostate cancer cells. J Cell Biochem 91:232–242
46. **Kolesnick RN, Kronke M** 1998 Regulation of ceramide production and apoptosis. Ann Rev Physiol 60:643–665
47. **Bu SZ, Blaukat A, Fu X, Heldin NE, Landstrom M** 2002 Mechanisms for 2-methoxyestradiol-induced apoptosis of prostate cancer cells. FEBS Lett 531: 141–151
48. **Haimovitz-Friedman A, Kolesnick RN, Fuks Z** 1997 Ceramide signaling in apoptosis. Brit Med Bull 53:539–553
49. **Ruvolo PP** 2003 Intracellular signal transduction pathways activated by ceramide and its metabolites. Pharm Res 47:383–392
50. **Mathias S, Pena LA, Kolesnick RN** 1998 Signal transduction of stress via ceramide. Biochem J 335:465–480
51. **Shimabukuro M, Zhou YT, Levi M, Unger RH** 1998 Fatty acid-induced β cell apoptosis: a link between obesity and diabetes. Proc Natl Acad Sci USA 95:2498–2502
52. **Schmitz-Peiffer C, Craig DL, Biden TJ** 1999 Ceramide generation is sufficient to account for the inhibition of the insulin-stimulated PKB pathway in C2C12 skeletal muscle cells pretreated with palmitate. J Biol Chem 274:24202–24210
53. **Boon H, Westlake K, Stewart M, Gray R, Fleshner N, Gavin A, Brown JB, Goel V** 2003 Use of complementary/alternative medicine by men diagnosed with prostate cancer. Urology 62:849–853
54. **Crescioli C, Villari D, Forti G, Ferruzzi P, Petrone L, Vannelli GB, Adorini L, Salerno R, Serio M, Maggi M** 2002 Des (1–3) IGF-I-stimulated growth of human stromal BPH cells is inhibited by a vitamin D-3 analogue. Mol Cell Endocrinol 198:69–75
55. **Cohen P** 1998 Serum insulin-like growth factor-I levels and prostate cancer risk—interpreting the evidence. J Natl Cancer Inst 90:876–879
56. **Chan JM, Stampfer MJ, Giovannucci E, Gann PH, Ma J, Wilkinson P, Hennekens CH, Pollak M** 1998 Plasma insulin-like growth factor I and prostate cancer risk: a prospective study. Science 279:563–566
57. **Wu SF, Sun HZ, Qi XD, Tu ZH** 2001 Effect of episteride on the expression of IGF-1 and TGF-β receptors in androgen-induced castrated rat prostate. Exp Biol Med 226:954–960
58. **Huynh H, Seyam RM, Brock GB** 1998 Reduction of ventral prostate weight by finasteride is associated with suppression of insulin-like growth factor I (IGF-I) and IGF-I receptor genes and with an increase in IGF binding protein 3. Cancer Res 58:215–218
59. **Huynh H, Alpert L, Alaoui-Lamali MA, Ng CY, Chan TWM** 2001 Co-administration of finasteride and the pure anti-oestrogen ICI 182,780 act synergistically in modulating the IGF system in rat prostate. J Endocrinol 171: 109–118
60. **Huynh H** 2002 Induction of apoptosis in rat ventral prostate by finasteride is associated with alteration in MAP kinase pathways and Bcl-2 related family of proteins. Int J Oncol 20:1297–1303
61. **Huynh H, Pollak M, Zhang JC** 1998 Regulation of insulin-like growth factor (IGF) II and IGF binding protein 3 autocrine loop in human PC-3 prostate cancer dells by vitamin D metabolite 1,25(OH)(2)D-3 and its analog EB1089. Intl J Oncol 13:137–143
62. **Majumder PK, Yeh JJ, George DJ, Febbo PG, Kum J, Xue Q, Bikoff R, Ma HF, Kantoff PW, Golub TR, Loda M, Sellers WR** 2003 Prostate intraepithelial neoplasia induced by prostate restricted Akt activation: the MPAKT model. Proc Natl Acad Sci 100:7841–7846

***Endocrinology* is published monthly by The Endocrine Society (http://www.endo-society.org), the foremost professional society serving the endocrine community.**